Energy & Environmental Science

Accepted Manuscript

ROYAL SOCIETY OF CHEMISTRY

www.rsc.org/ees

Energy Environ. Sci.

RSCPublishing

COMMUNICATION

Reversible Br_2/Br^- Redox Couple in Aqueous Phase as High-performance Catholyte for Alkali–ion Batteries†

Cite this: DOI: 10.1039/x0xx00000x

Yu Zhao,‡ Yu Ding,‡ Jie Song, Lele Peng, John B. Goodenough, and Guihua Yu*

Received 00th January 2014,
Accepted 00th February 2014

DOI: 10.1039/x0xx00000x

www.rsc.org/ees

An aqueous catholyte of a Li–ion redox battery employing reversible Br_2/Br^- redox reactions is investigated. The catholyte uses lithium bromide as active material and potassium bromide aqueous solution as supporting electrolyte. By tuning the acidity of the catholyte, stable cyclability of the cell has been achieved at room temperature with discharge potential ~3.9 V, reversible capacity of 290 mA h g^{-1}, and specific power density ~1000 W kg^{-1}. Compared with the catholytes used in conventional redox-flow batteries, the reported catholyte is heavy-metal-free and can be operated in moderate acidity, providing an alternative option for sustainable electrical energy storage.

Broader context

Electrical energy storage in secondary batteries is the principle power source for electric vehicles and sustainable energies such as wind and solar power. Increasing the energy/power density, energy efficiency and the life-span of secondary batteries at an affordable cost are critical for practical applications. These parameters are, in turn, controlled by the battery-component materials and their fabrication costs. Halogens, such as iodine and bromine, show their potential towards rechargeable alkali-ion batteries owing to their relatively low molecular weight, high solubility and reversible redox reaction of X_2/X^- (X = I, Br) in liquid phase. An aqueous catholyte operating via the rapid Br_2/Br^- redox reaction yields high discharge potential and power density, making it as a potential candidate that combines the concept and advantage of Li–ion batteries and redox-flow systems, and steps further beyond the conventional intercalation electrode materials and the conventional redox-flow batteries.

Renewable energy resources are expected to make important contributions to provide environment-friendly solutions of the energy problem. Renewable energy from sunlight and wind, however, is intermittent and frequently unpredictable regarding their availability, thus limiting its utility as a direct and reliable power supply. Consequently, the development of more potential renewable energy resources and the integration of those resources efficiently into an electrical-energy storage for the grid create a pressing need for the development of energy storage systems.[1, 2] Rechargeable batteries provide a simple and efficient way to store electricity for a wide range of applications, from small portable electronics, transportation, to grid energy storage. Intrinsically, alkali–ion batteries, Li–ion batteries for example, exhibit a higher gravimetric energy density over lead–acid, Ni–Cd, or Ni–MH batteries. However, it seems to be problematic to simply scale up the insertion chemistry of traditional Li–ion batteries because of the limitation in accommodating guest Li^+ ions within the host cathode materials.[3] The nonaqueous Li–S and $Li–O_2$ batteries promise high energy density, but limitations remain owing to the relatively low discharging potential of the sulphur (2.4 − 2 V *vs.* Li^+/Li) and large over potential of the $Li–O_2$ batteries.[4] Accordingly, further development in battery technology relies on more radical approaches, such as developing new-concept alkali–ion batteries that utilize an alternative chemistry or designing new prototype batteries that employ varied combinations of electrode couples as well as electrolytes.[5] Recently, several strategies for Li–ion batteries using a soluble redox couple as the catholyte have been proposed.[6–15] Particularly, aqueous catholytes simply use water as solvent with much higher Li^+ diffusion coefficient than intercalation materials, and they can be easily circulated in a flow-through configuration.[7] Combining the existing knowledge of alkali–ion batteries with the advantage of redox-flow

Materials Science and Engineering Program and Department of Mechanical Engineering, The University of Texas at Austin, Austin, TX 78712, USA. Email: ghyu@austin.utexas.edu

† Electronic Supplementary Information (ESI) available. See DOI: 10.1039/c000000x/

‡ These authors contributed equally to this work

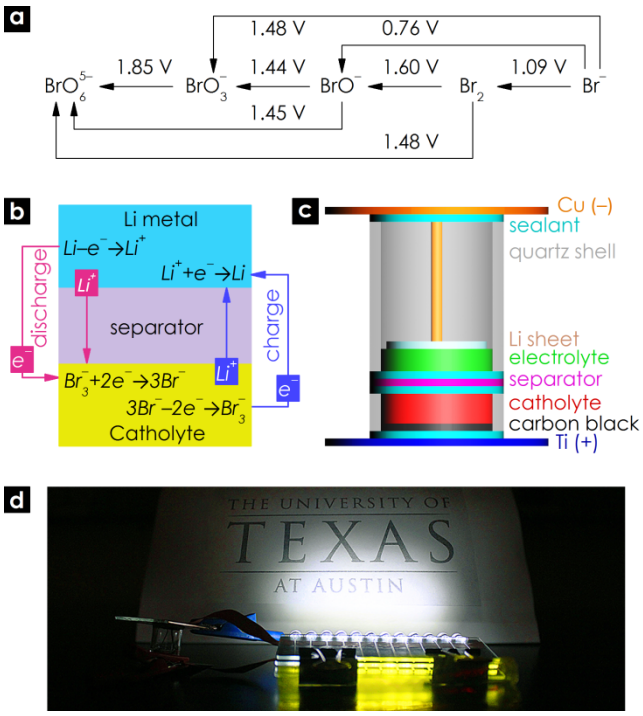

Fig. 1 Design principle of the Br_2/Li half-cell. (a) Standard redox potential of Br at its various valence states. All the redox potentials are standard values with respect to SHE. (b) The working principle of the half-cell. (c) Cell structure used for the electrochemical characterization of the Br_2/Br^- catholyte. (d) An experimental demonstration of the power output of the Br_2/Br^- catholyte.

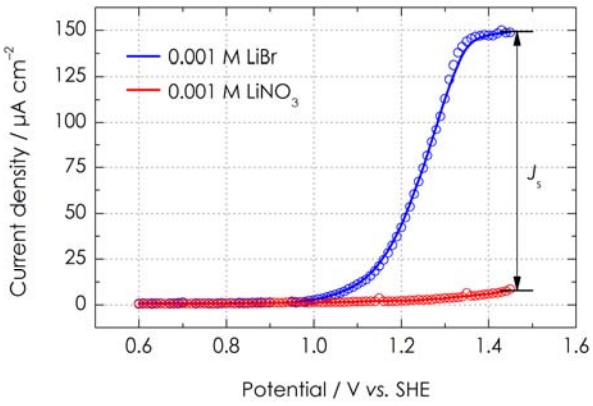

Fig. 2 Sampled-current voltammogram profile of LiBr aqueous solution (blue) for the determination of the diffusion coefficiency and oxidative rate constant of Br^-. The sampled-current voltammogram profile of $LiNO_3$ aqueous solution (red) was also measured as background in consideration of possible O_2 evolution at high potential.

systems, the aqueous catholyte shows the benefit of decoupling energy content and power output, both of which are independently scalable.[16]

A potential alkali-ion catholyte should take into consideration the specific capacity and proper redox potential. In theory, the stable electrochemical potentials of aqueous electrolyte solutions at neutral pH should be in the potential window of −0.4 − 0.83 V (*vs.* SHE, standard hydrogen electrode) based on the Nernst equation. Water electrolysis, however, would not generally proceed beyond these terminal potentials, as the electrical input must provide the full amount of enthalpy of H_2/O_2 evolution, which broadens the threshold of water electrolysis to *ca.* −0.75 − 1.25 V (*vs.* SHE) or 2.29 − 4.29 V (*vs.* Li^+/Li).[15] Therefore, it's possible to use those redox couples that with high redox potential in the aqueous phase to achieve a Li−ion catholyte with maximized operation potential. **Table S1** summarizes some redox couples that show potential for the design of aqueous and/or nonaqueous catholytes for electrical energy storage. The redox potential and molecular weight of the redox species are two major concerns in turn to achieve high potential and high capacity. Compared with the reported catholytes, bromine shows a redox potential *ca.* 4.1 V (*vs.* Li^+/Li) within the potential range of water electrolysis, specific capacity of 331.2 mA h g^{-1}, and acceptable solubility with the co-existence of bromide *via* the reaction of $Br_2 + Br^- \rightarrow Br_3^-$. Herein, we report an aqueous catholyte based on the reversible Br_2/Br^- redox reaction, which shows discharge potential between 3.9 − 4.1 V (*vs.* Li^+/Li). In addition, the high specific capacity, stable cyclability and energy efficiency make this catholyte a low-cost electric energy storage medium.

The feasibility of using Br_2/Br^- redox reactions to design the aqueous catholyte is revealed in **Fig. 1a**, in which the redox potentials at different valence states of Br are presented.[17] Theoretically, Br^- can be oxidized into Br_2 or BrO^- below the O_2 evolution potential. The oxidation of Br^- into BrO^-, however, only proceeds smoothly in basic environment. Tuning the pH value of the catholyte into weak acidic can reduce the concentration of OH^-, resulting in suppressed oxidation of Br^- into BrO^-. Therefore, it's possible to take advantage of the redox reaction of Br_2/Br^- as the sole or dominant reaction in the catholyte during charge/discharge as illustrated in **Fig. 1b**. A water-stable solid electrolyte plate was used to separate the aqueous catholyte from the organic electrolyte in the anode. The solid electrolyte showed reasonable stability towards neutral or weak acidic aqueous solution,[9] but would be less stable in strong acidic or basic environment.[18] A cylinder-type cell was used to evaluate the electrochemical performance of the catholyte. **Fig. 1c** shows the cell structure in which the catholyte is separate from a conventional anode by a Li−ion conducting membrane (NASICON-type $Li_{1+x+3z}Al_x(Ti,Ge)_{2-x}Si_{3z}P_{3-z}O_{12}$). The cathode part is composed of acetylene black as current collector, Ti foil as supporting substrate, and KBr/LiBr aqueous solution as the catholyte (LiBr loading amount ~ 5.5 mg cm^{-2}, pH 4.5 − 5, adjusted with diluted sulphuric acid). The anode part is composed of conventional organic electrolyte (1M $LiPF_6$ in ethylene carbonate/diethyl carbonate), Li metal and Cu as the current collector (detailed fabrication process can be found in the Methods part and **Fig. S1**, ESI†). A demonstration of the power output of the half-cell is shown in **Fig. 1d**. The fully charged half-cell with an area of solid electrolyte of 9 mm in diameter showed a power output high enough to light 12 LED bulbs simultaneously.

Sampled-current voltammogram was first carried out on the catholyte to estimate the diffusion coefficient and redox kinetics which are the key factors to achieve high performance. **Fig. 2** shows the sampled-current voltammogram profile of alkali bromide solution on acetylene black/PVDF surface. Equation (1) was used

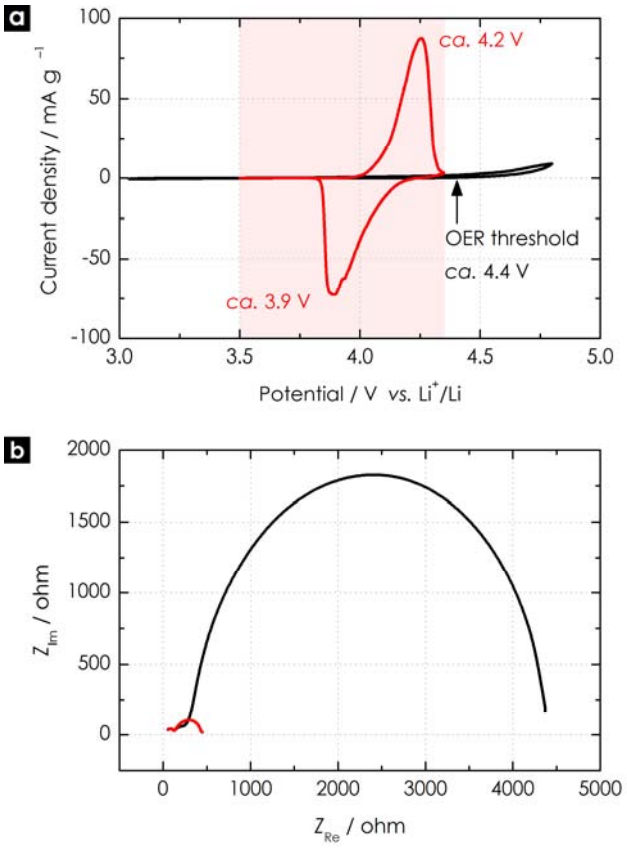

Fig. 3 Determination of the working conditions of the half-cell. (a) CV curves of the Br_2/Br^- catholyte (red) and Li_2SO_4 aqueous solution (black) at pH 4.5 – 5. (b) Nyquist plots of the as-assemble cell (black) and the cell after initial charge/discharge cycle.

to estimate the diffusion coefficient (D) of Br^- at the given concentration:[19]

$$D = \frac{J_s^2 \pi t}{n^2 F^2 C^2} \quad (1)$$

where J_s is the steady-state current, F is Faraday constant, t = 3s, and C is the bulk concentration of Br^- (10^{-6} mol cm^{-3}). The Br^- diffusion coefficient was determined to be ~ 2 × 10^{-5} cm^2 s^{-1}, which is consistent with the standard value (D_0 = 2.08 × 10^{-5} cm^2 s^{-1}):[20]

$$k_0 = \frac{D_0^{1/2}}{\pi^{1/2} t^{1/2}} \exp\left(\frac{nF}{RT} | E_{1/2} - E_0 |\right) \quad (2)$$

The kinetic redox rate constant k_0 was found to be ~ 6 × 10^{-3} cm s^{-1} calculated from equation (2), where n is the number of electrons transferred per ion, R is the universal gas constant, T is temperature in kelvin, $E_{1/2}$ is the corresponding potential at half of the steady-state current at 1M Br^- (1.136 V *vs.* SHE, **Fig. S2**, ESI†), and E_0 is the standard redox potential of Br_2/Br^- (1.09 V *vs.* SHE).[17] The rate constant is greater than the rate constant on vitreous carbon, and the rate constants of other species used in flow batteries such as VO_2^+/VO^{2+}, Fe^{3+}/Fe^{2+}, Ce^{4+}/Ce^{3+} and Cr^{3+}/Cr^{2+}.[21] The high diffusion coefficient together with the rapid redox kinetics implies that the voltage loss due to the rate of surface electrochemical reactions is negligible. The high rate is due to high diffusion coefficiency of Br^- in the catholyte and sufficient electrochemical activity of Br_2/Br^- redox reaction on the activated carbon surface.

The electrochemical processes involved in the Br_2/Br^- catholyte were revealed by cyclic voltammetry (CV). **Fig. 3a** shows the CV curve of the cylinder half-cell in the potential window of 3.5 − 4.35 V (*vs.* Li^+/Li). The cathodic and anodic peaks were centred at the potential of *ca.* 4.2 and *ca.* 3.9 V (*vs.* Li^+/Li), corresponding to the redox potential of Br_2/Br^- in the aqueous phase. Furthermore, the integrated areas of the cathodic and anodic scans were identical, suggesting that the redox reaction between Br^- and Br_2 was the sole reaction in the catholyte. The practical threshold of O_2 evolution reaction (OER, **Fig. S3**, ESI†) potential should be higher than 4.4 V at pH 5 (*vs* Li^+/Li), while H_2 evolution reaction (HER) could only take place at the potential lower than 3.04 V (*vs.* Li^+/Li). Thus, neither O_2 nor H_2 evolution were likely to take place on the acetylene black in the potential window of 3.5 − 4.35 V (*vs.* Li^+/Li). The resistances from the catholyte and interfaces between the catholyte/current collector and catholyte/solid electrolyte were small according to the electrochemical impedance spectroscopy (EIS) analysis shown in **Fig. 3b**. The fitted values (the corresponding equivalent circuits was shown in **Fig. S4**, ESI†) of the contributions from the electric resistance (R_e), charge-transfer resistance (R_{ct}), grain-boundary resistance (R_{gb}) and interfacial resistance (R_{int}) are summarized in **Table S2**. Owing to the hydrophobic nature of the acetylene black/PVDF, the contact area between the catholyte and the current collector was limited, resulting in a huge interfacial resistance. The formation of hydrophilic groups on the surface of the acetylene-black/PVDF film during the initial cycle led to better wettability of the current collector (**Fig. S5**, ESI†) and thus resulted in a decreased interfacial resistance. The resistances from the electrode and charge-transfer remained almost constant after initial cycle. Therefore, a current collector with better wettability and higher surface area would contribute, in turn, to minimize the interfacial resistance and accelerate the charge transfer between the liquid and solid interface. The grain-boundary resistance, which dominated the total resistance of the cell, mainly arose from the tape-casted solid electrolyte, and kept nearly constant upon cycling.

The discharge behaviour of the Br_2/Br^- catholyte to estimate its power density was first characterized by the polarization curve. The catholyte could work safely at room temperature at a specific power density of *ca.* 980 W kg^{-1} achieved at current density of 335 mA g^{-1} (330 mA g^{-1} = 1C) and discharge potential of ~ 3 V (*vs.* Li^+/Li), while the peak power output was *ca.* 1600 W kg^{-1} as indicated in **Fig. 4a**. The specific power density was greater than conventional rechargeable batteries such as lead−acid, Ni−Cd, or Ni−MH, and was comparable to that of Li−ion batteries.[22] The gradual potential drop with the increase of current densities indicates a mass-transport loss dominated by the slow mobility of Li^+ ions in the solid electrolyte; the reduction of Br_2 on activated carbon exhibits negligible polarization at an even higher current rate.[23] Increasing the conductivity of the solid electrolyte by means of increasing the temperature gives the further improvement of the power density. For example, the catholyte exhibited specific power density of 1790/3230 W kg^{-1} at current density of 630/1000 mA g^{-1}

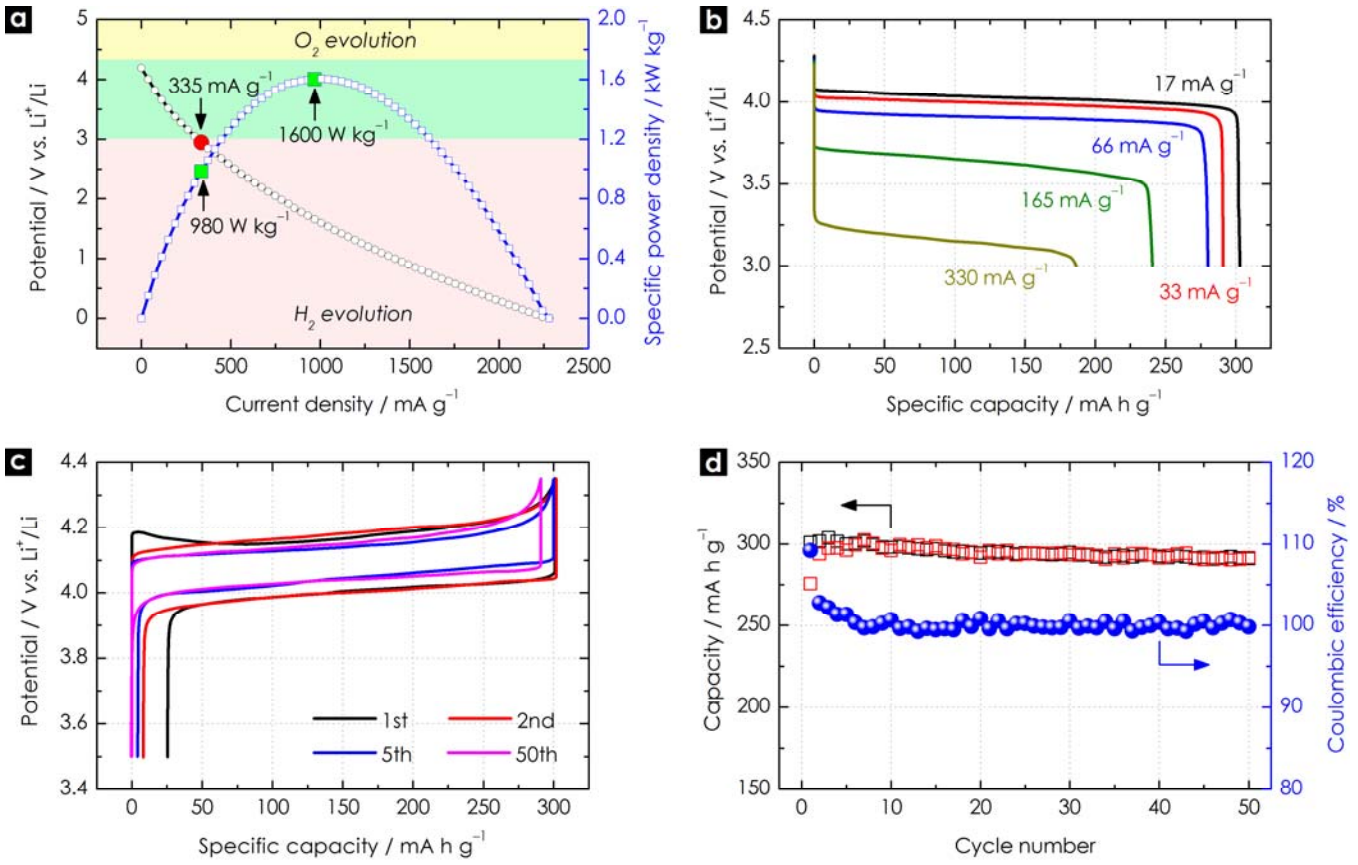

Fig. 4 Electrochemical performance of the half-cell. (a) Polarization curve (black) and corresponding specific power density (blue) at room temperature. (b) Discharge behaviour at various current densities. All the cells were fully charged to 4 .35 V (vs. Li^+/Li) before test. (c) Representative charge/discharge profiles and (d) charge/discharge capacity with corresponding Coulombic efficiency at room temperature over cycling. Black and red squares refer to the charge and discharge capacities, respectively.

and peak power output of 2880/4740 W kg^{-1} at 40/55 °C, respectively (**Fig. S6** and **S7,** ESI†). The Br_2/Br^- catholyte was also fully discharged at various current densities of 17 − 330 mA g^{-1} (0.05 − 1C). A higher current density was not applied due to the low conductivity of the solid electrolyte and safety issues such as H_2 evolution and structural distortion of the solid electrolyte. The Br_2/Br^- catholyte delivered a capacity of 303 mA h g^{-1} at 17 mA g^{-1} with a broad plateau around 4 V, and maintained a capacity of 185 mA h g^{-1} at 330 mA g^{-1} with a discharge potential around 3.1 V as shown in **Fig. 4b**. As the current density increases, both the ohmic polarization, which mainly resulted from the resistance of the solid electrolyte, and the concentration polarization, which arose from both limited Li−ion transport capabilities from the solid electrolyte and Br_2 diluent, became more obvious. However, the Br_2/Br^- redox reaction on activated carbon, such as acetylene black, usually exhibits high activity and rapid reaction kinetics.[24] The bottleneck of the rate capability should be attributed to the relatively low conductivity of the solid electrolyte (~10^{-4} S·cm^{-1} at room temperature)[25] compared to that of Li^+ or Br^- in the aqueous phase (~10^{-2} S·cm^{-1}),[20] and that of Li^+ in the organic electrolyte (~10^{-3} S·cm^{-1}).[26] It could be expected that the development of solid electrolytes with superior conductivity as well as robust mechanical property and chemical stability would further enhance the performance of the cell.

The cyclability and stability of the Br_2/Br^- catholyte were examined by galvanostatic charge/discharge. The current density was set to 33 mA g^{-1} (0.1C) between 3.5 − 4.35 V (*vs.* Li^+/Li) in consideration of the low conductivity of the solid electrolyte. The representative charge/discharge profiles of selected cycles were presented in **Fig. 4c**. The Br_2/Br^- catholyte gave a discharge potential above 3.9 V (*vs.* Li^+/Li), higher than that of the reported catholytes.[5–10, 27] The reversible capacity reached *ca.* 290 mA h g^{-1}, 88% of theoretical capacity. Since it was necessary to retain traces of Li^+ in the catholyte to sustain the applied current, the specific capacity during initial charging (301 mA h g^{-1}) was smaller than the theoretical capacity of Br_2 (331.2 mA h g^{-1}). A certain amount of Br_2 was also retained during the initial discharge in order to sustain the applied current, which prevented to taking full use of the active material. The charge/discharge capacity was stable in the measured cycles with capacity decay less than 1‰ per cycle, and the Coulombic efficiency after the first few cycles was ~ 100% as summarized in **Fig. 4d**. It should be pointed out that the obvious over potential at the beginning of the 1st charging process was due to the large interfacial resistance for mass transport between the catholyte and the hydrophobic acetylene black/PVDF current collector. Upon cycling, the surface of acetylene black/PVDF showed better hydrophilicity, which allowed more sites for Br_2/Br^- reduction/oxidation thus contributing to decrease the over potential.

For instance, the over potential of the 5th cycle was 80 mV lower than that of the 1st cycle.

The pH value plays an important role in determining the cyclability of the Br_2/Br^- catholyte. Weak or moderate acidic environment would help to supress the formation of BrO^- while maintain the stability of the solid electrolyte. The catholyte with weak or moderate acidity showed better performance in terms of cyclability and stability of discharge potential than those with pH ~ 8.5 (as-prepared) and neutral pH value (adjusted with diluted sulphuric acid). For the as-prepared catholyte, the formation of BrO^-, which could not be reversibly reduced to Br^- in basic environment, would decrease its cyclability. The discharge potential decreased from *ca.* 3.9 V to *ca.* 3.4 V upon cycling (**Fig. S8**, ESI†) while the charge potential remained unchanged probably due to the excess Br^- in the catholyte. Neutral environment (pH 6.5 − 7) could partially suppress the formation of BrO^-, but not sufficiently. The discharge potential in neutral environment still decreased from *ca.* 4 V to *ca.* 3.7 V upon cycling (**Fig. S9**, ESI†). The catholyte showed a similar performance under moderate acidity (pH 3 – 3.5, **Fig. S10**, ESI†) compared with that under weak acidity (pH 4.5 – 5, **Fig. 4c**). It's reported that when exposed to strong acidity, the solid electrolyte underwent gradual decomposition. However, little conductivity change was observed when exposed to moderate acidity (pH 3.3).[28] The weak or moderate acidity of the catholyte in this study showed little effect on the long-term stability the solid electrolyte as evident by the unchanged crystal structural (**Fig. S11**, ESI†) and ionic conductivity (**Fig. S12**, ESI†) when exposed to the catholyte for sufficient time.

It's of noting that the Li−ion diffusion across the solid electrolyte is more favourable in neutral environment, and other than Li−ions, hydrated protons cannot pass through the solid electrolyte as evident by the EIS analysis (**Fig. S13**, ESI†). In addition, the ionic conductivity of the solid separator needs to be increased in low temperature range. The development of super-ionic conductors with acceptable ionic conductivity, mechanical robustness, and chemical stability challenges the practical application for the Br_2/Br^- catholyte in sustainable electric energy storage. Moreover, the separator needs to block dendrites from a metallic-alkaline anode without being reduced. Alternative ways are to use commercially available graphite to make a semi-flow cell, or to use small soluble organic molecules with suitable redox potential and solubility to form the corresponding anolyte to operate the cell in a complete flow-through mode to offer an energy density comparable to conventional secondary batteries. Note that an energy density of ~ 100 W h kg^{-1} without a cathode-flow-through mode can be expected given the saturated concentration of Br_2 in aqueous phase of ~ 2 M.[9] Compared with the reported Li-redox batteries based on other reversible redox reactions in aqueous/liquid phase,[6, 8, 9, 12, 15, 29] the Br_2/Br^- catholyte shows a high discharge potential with large reversible capacity (**Fig. S14**, ESI†). Meanwhile, advanced structural design of the battery components would benefit the performance improvement.[30] Also, sodium might be used as the anode instead of lithium, which can further decrease the cost of a full cell.

Conclusions

In conclusion, the reversible Br_2/Br^- redox couple in aqueous phase shows its potential for the design of Li−ion flow batteries for sustainable electrical energy storage. The Br_2/Br^- catholyte simply uses alkali bromide aqueous solution, which serves as both electrolyte and active material. The Br_2/Br^- catholyte/Li half-cell shows a high discharge potential around 4 V at 0.1C with stable capacity retention, and delivers a reversible capacity *ca.* 290 mA h g^{-1}, and a specific power density nearly 1000 W kg^{-1} at room temperature. Optimization of engineering and operating parameters such as flow-battery design, electrode design, and conductivity enhancement of the solid electrolyte should lead to significant performance improvements in the future.

Methods

Materials.

All chemicals were used as received. Potassium bromide (KBr, 99.5%), lithium bromide (LiBr, 99.9%, anhydrous), titanium foil (100 μm thick, 99.5%), copper foil (30 μm thick, 99.5%), copper mesh (100 mesh, 99.6%), acetylene black, polyvinylidene fluoride binder (PVDF), and N-methyl-2-pyrrolidone (NMP) were purchased from Fisher Scientific. The solid electrolyte (tape casted, ionic conductivity: 3×10^{-4} S·cm^{-1} at 298K) was purchased from Ohara Corporation. Organic electrolyte (1M $LiPF_6$ in ethylene carbonate (EC)/diethyl carbonate (DEC) with volume ratio of 1:1) was purchased from BASF. The sealant (Meltonix 1170−25PF) for battery module assembly was from Solaronix.

Preparation of the cylinder cell module & current collector.

The cylinder cell was made from two quartz cylinders with outer diameter of 12 mm and inner diameter of 10 mm. The height of quartz cylinder was 1.7 mm for the cathode compartment and 10 mm for the anode compartment. Acetylene black was used as current collector and titanium foil was used as supporting substrate in the cathode part. One hole as the inlet for injection of the catholyte was made on titanium foil prior to casting the carbon slurry on the supporting titanium foil. The carbon slurry used as current collector was prepared in Thinky ARE-310 by mixing acetylene black, PVDF and NMP in the weight ratio of 9: 1: 90. The geometric area of the casted slurry was 9 mm in diameter. The typical loading amount of acetylene black/PVDF mixture was ~ 0.5 mg cm^{-2}. The as-prepared current collector was dried at 115 °C in vacuum for 12 h to remove residual NMP and further annealed at 150 °C for 1 h for better adhesion to the titanium foil.

Cell assembly.

Schematic illustration of the fabrication process is shown in **Fig. S1**. There were three major steps involved: i) the fabrication of the module of the cylinder cell; ii) the fabrication of the anode part, which was carried out in glove box with water concentration less than 2 ppm; and iii) the fabrication of the cathode part. For the fabrication of the module of the cylinder cell, the as-prepared current collector, cylindrical quartz shells and solid electrolyte were

sealed together with the sealant. The fabrication of the anode part was conducted in glove box. A piece of Li sheet was pressed onto the copper mesh which was welded onto a copper foil. After injection of the organic electrolyte, the cylindrical quartz shell of the anode part was covered by the copper foil and sealed hermetically. The fabrication of the cathode part was carried out in ambient conditions. An aqueous solution containing 1M KBr and 0.3M LiBr (pH 4.5 − 5, adjusted by sulphuric acid) was injected through the hole on the titanium foil into the cylindrical quartz shell on the cathode part. The hole was sealed by Kapton ® tapes.

Characterization.

Sampled-current voltammogram was carried out in LiBr solution (pH 4.5 − 5, adjusted with sulphuric acid) with acetylene black/PVDF coated on titanium foil as the working electrode, titanium foil as the counter electrode. 0.001 M LiBr aqueous solution was used to measure the diffusion coefficient of Br^- (D), while 1M LiBr aqueous solution was used to determine the kinetic redox rate constant (k_0) on acetylene black/PVDF electrode. To make the surface of acetylene black/PVDF film hydrophilic, the working electrode was first oxidized in the 1 mM LiBr solution by CV scanning at 5 mV s^{-1} in the potential range of 3.5 − 4.35 V (*vs.* Li^+/Li). Sufficient CV cycles were necessary to achieve a hydrophilic surface of the working electrode. The CV, EIS, polarization curve and galvanostatic charge/discharge measurements were carried out on a BioLogic VMP3 potentiostat equipped with impedance modules. CV measurements for Br_2/Br^- catholyte and Li_2SO_4 aqueous solution were carried out in the potential window of 3.5 − 4.35 V (*vs.* Li^+/Li) and 3 − 4.8 V (*vs.* Li^+/Li), respectively, at a sweeping rate 0.02 mV s^{-1}. The frequency region for EIS measurements was set to 10^6 − 1 Hz. Rate capability and cyclic performance were carried out in the potential window of 3 − 4.35 V and 3.5 − 4.35 V (*vs.* Li^+/Li), respectively. XRD measurement was performed on a Philips APD 3520 X-ray diffractometer with Cu Kα radiation in steps of 0.02º with a step time of 4 s over the 2θ range.

Acknowledgements

G.Y. acknowledges the financial support from the start up grant from Cockrell School of Engineering at the University of Texas at Austin. J.B.G. acknowledges the support by the Robert A. Welch Foundation of Houston, Texas.

Notes and references

1 B. Dunn, H. Kamath and J.-M. Tarascon, *Science*, 2011, **334**, 928−935.
2 Z. G. Yang, J. L. Zhang, M. C. W. Kintner-Meyer, X. C. Lu, D. W. Choi, J. P. Lemmon and J. Liu, *Chem. Rev.*, 2011, **111**, 3577−3613.
3 M. R. Palacín, *Chem. Soc. Rev.*, 2009, **38**, 2565−2575.
4 P. G. Bruce, S. A. Freunberger, L. J. Hardwick and J.-M. Tarascon, *Nat. Mater.*, 2012, **11**, 19−29.
5 Y. Wang, P. He and H. Zhou, *Adv. Energy Mater.*, 2012, **2**, 770−779.
6 Y. Wang, Y. Wang and H. Zhou, *ChemSusChem*, 2011, **4**, 1087−1090.
7 Y. Lu and J. B. Goodenough, *J. Mater. Chem.*, 2011, **21**, 10113−10117.
8 Y. Lu, J. B. Goodenough and Y. Kim, *J. Am. Chem. Soc.*, 2011, **133**, 5756−5759.
9 Y. Zhao, L. Wang and H. R. Byon, *Nat. Commun.*, 2013, **4**, 1896.
10 B. Huskinson, M. P. Marshak, C. Suh, S. Er, M. R. Gerhardt, C. J. Galvin, X. Chen, A. Aspuru-Guzik, R. G. Gordon and M. J. Aziz1, *Nature*, 2014, **505**, 195−198.
11 Y. Zhao and H. R. Byon, *Adv. Energy Mater.*, 2013, **3**, 1630−1635.
12 H. Senoh, M. Yao, H. Sakaebe, K. Yasuda and Z. Siroma, *Electrochim. Acta*, 2011, **56**, 10145−10150.
13 N. F. Yan, G. R. Li and X. P. Gao, *J. Mater. Chem. A*, 2013, **1**, 7012−7015.
14 Y. Yang, G. Zheng and Y. Cui, *Energy Environ. Sci.*, 2013, **6**, 1552−1558.
15 L. Chen, Z. Guo, Y. Xia and Y. Wang, *Chem. Commun.*, 2013, **49**, 2204−2206.
16 P. J. Cappillino, H. D. Pratt III, N. S. Hudak, N. C. Tomson, T. M. Anderson and M. R. Anstey, *Adv. Energy Mater.*, 2014, **4**, 1300566.
17 J. A. Dean, *Lange's Chemistry Handbook*, 14th ed., McGraw-Hill Professional Publishing, New York, 1992.
18 T. Zhang, N. Imanishi, S. Hasegawa, A. Hirano, J. Xie, Y. Takeda, O. Yamamoto and N. Sammes, *J. Electrochem. Soc.*, 2008, **155**, A965−A969.
19 A. J. Bard and L. R. Faulkner, *Electrochemical Methods, Fundamentals and Applications*, Wiley, New York, 1980.
20 D. R. Lide, *CRC Handbook of Chemistry and Physics*, 3rd electronic edition, CRC Press, LLC, Boca Raton, FL, 2000.
21 A. Z. Weber, M. M. Mench, J. P. Meyers, P. N. Ross, J. T. Gostick and Q. Liu, *J. Appl. Electrochem.*, 2011, **41**, 1137−1164.
22 P. Simon and Y. Gogotsi, *Nat. Mater.*, 2008, **7**, 845−854.
23 H. S. Lim, A. M. Lackner and R. C. Knechtli, *J. Electrochem. Soc.*, 1977, **124**, 1154−1157.
24 L. Zhang, H. Zhang, Q. Lai, X. Li and Y. Cheng, *J. Power Sources*, 2013, **227**, 41−47.
25 http://www.oharacorp.com/lic-gc.html (accessed in March 2014).
26 K. Xu, *Chem. Rev.*, 2004, **104**, 4303−4417.
27 W. Wang, Q. Luo, B. Li, X. Wei, L. Li, and Z. Yang, *Adv. Funct. Mater.*, 2013, **23**, 970−986.
28 T. Zhang, N. Imanishi, Y. Shimonishi, A. Hirano, Y. Takeda, O. Yamamoto and N. Sammes, *Chem. Commun.*, 2010, **46**, 1661−1663.
29 Y. Wang and H. Zhou, *Electrochem. Commun.*, 2009, **11**, 1834−1837.
30 Y. Zhao, M. Hong, N. Bonnet-Mercier, G. Yu, H. C. Choi and H. R. Byon, *Nano Lett.*, 2014, **14**, 1085−1092.

TOC graphic

An aqueous catholyte based on sole bromine/bromide redox couple shows operating potential ~4 V, reversible capacity of 290 mA h g^{-1}, and specific power density approaching 1000 W kg^{-1}, making it a potential candidate for sustainable electrical energy storage.